Time-Frequency Signatures of a Moving Target in SAR Images

Trygve Sparr
Norwegian Defence Research Establishment (FFI)
Land and Air Systems Division
PO Box 25, NO-2027 Kjeller
NORWAY

Trygve.Sparr@ffi.no

SUMMARY

Moving targets within SAR scenes are distorted depending on the particulars of the target motion. For small motions, the uncompensated phase of a point reflector is a sum of a term proportional to the range component of the target motion, and a more complicated term depending on the azimuth motion. The resulting phase may be analysed with time-frequency techniques since the motion effect may alternatively be seen as a time dependent Doppler frequency. An experiment performed with a moving target within a scene collected by the German E-SAR system gave a signature that agrees well with theoretical predictions. Time-frequency analysis, using the smoothed pseudo Wigner-Ville method, gave a linear chirp with superimposed oscillations as predicted from the theory and the target motion.

1.0 INTRODUCTION

Synthetic aperture radar (SAR) is a useful radar technique to generate images of a scene with fairly high resolution from standoff ranges. SAR imaging of stationary scenes is well understood theoretically [1], and the major issue is the speed and accuracy of the SAR processor. For a moving target within the scene, the situation is more complicated. On the one hand, it is easier to detect the target using techniques different form SAR [2]. On the other hand, target motion results in image distortion in the SAR image of the target itself. A well known example is the azimuth displacement of a target with a small constant range rate. More complicated motion leads to other effects. Vibrations and rotations cause micro-Doppler [3], and azimuth smearing may result [4].

We analyse the effect of general target motion on the SAR signal phase. For reasonably small motions, the residual uncompensated phase of a moving point target after the SAR processor consists of two terms, one proportional to the range component of the motion, and one containing the product of the platform motion and the target azimuth motion. This phase can be complicated, and time-frequency methods are useful for the analysis.

An experiment was performed in Lillestrøm, Norway, using the DLR E-SAR from Germany as SAR platform. A moving target with a known motion was present at the time of data collection. The motion was an approximately constant range rate, with an oscillation in the range direction superimposed. Results obtained with time frequency methods agreed well with theoretical predictions.

2.0 MOVING TARGETS IN SAR IMAGES

SAR processors usually assume that the scattering centres within the SAR scene are stationary during the time of data collection. Each point within the scene is then characterized by a unique phase history, and the SAR processor exploits the uniqueness to place the point within the scene.

Paper presented at the RTO SET Symposium on "Target Identification and Recognition Using RF Systems", held in Oslo, Norway, 11-13 October 2004, and published in RTO-MP-SET-080.

2.1 General Motion

We consider a SAR platform moving along a straight line with constant platform velocity v_p. We define the straight line as the x-axis in a cylindrical coordinate system as in [1]. At the time $t = 0$ the radar antenna phase centre is at the origin. At the same time, a target is exactly broadside at the range $d = r_0$. The target has a general motion described by its cylindrical coordinates $s(t)$ as given in fig. 1.

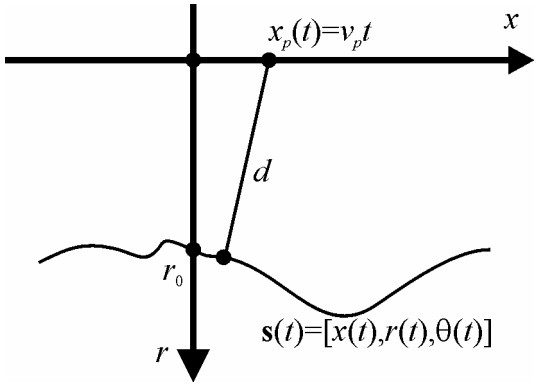

Figure 1: Geometry of a SAR system with a moving target.

Accordingly, the range from the radar to the target at a general time is given by

$$d(t) = \sqrt{\left[v_p t - x(t)\right]^2 + r^2(t)}\,. \tag{1}$$

The usual hyperbolic expression for the point target range history is obtained for $x(t) = 0$ and $r(t) = r_0$. Note that the cylindrical angle θ does not enter the equations as it does not affect the range when the platform trajectory is a straight line. The phase history of the target may then be obtained from

$$\varphi(t) = 2kd(t) = \frac{4\pi}{\lambda} d(t)\,. \tag{2}$$

Ideally, the SAR processor focuses the target using the phase history

$$\varphi_0(t) = \frac{4\pi}{\lambda} d_0(t) = \frac{4\pi}{\lambda} \sqrt{v_p^2 t^2 + r_0^2}\,. \tag{3}$$

Accordingly, the uncompensated phase may be found as

$$\Delta\varphi(t) = \varphi(t) - \varphi_0(t)\,. \tag{4}$$

Depending on the particulars of the motion, the uncompensated phase may result in a wide range of phenomena, from a simple shift in position of the target to a smearing making the target impossible to see.

2.2 Small Motions

Equations (1) to (4) give the general results, but are difficult to analyse directly. If the synthetic aperture is sufficiently short as compared to the distance to the scene, and the target motion is slow as compared to

the platform velocity, the square roots may be approximated by parabolas in the usual way [1]. The results are

$$d(t) \approx r_0 + \frac{v_p^2 t^2}{2r_0} - \frac{x(t)v_p t}{r_0} + \Delta r(t)$$
$$d_0(t) \approx r_0 + \frac{v_p^2 t^2}{2r_0} \tag{5}$$

Here, $\Delta r(t) = r(t) - r_0$, which is much smaller than r_0 under the stated conditions. Accordingly, the phase residual is given by

$$\Delta\varphi(t) \approx \frac{4\pi}{\lambda}\Delta r(t) - \frac{4\pi x(t)v_p t}{\lambda r_0}. \tag{6}$$

Note that for $x(t) = x_0$, a constant, the expression corresponds to the azimuth shift linear phase ramp to move the reflector to the new position when $\Delta(r) = 0$. On the other hand, when neglecting the second term and setting $\Delta r(t) = v_r t$, we get an azimuth phase ramp corresponding to the well known azimuth shift of a target with a moderate constant range rate v_r. A target moving with a constant azimuth rate will however introduce a quadratic phase term, resulting in smearing of the target.

3.0 TIME-FREQUENCY ANALYSIS

The phase residual as calculated in the previous section, given in eq. (6), may alternatively be seen as a Doppler shift. The basis is to define the corresponding Doppler frequency as

$$f_d = \frac{1}{2\pi}\frac{\mathrm{d}\varphi}{\mathrm{d}t}. \tag{7}$$

We see then that a linear phase ramp becomes a constant frequency, while the quadratic phase corresponding to constant azimuth rate becomes a linear chirp. For complicated frequency dependencies, time-frequency methods can be used for analysis.

3.1 Quadratic Time-Frequency Methods

There is a large number of different time-frequency methods that may be applied to a particular problem, and it is not always obvious which one to choose. The Cohen's class of quadratic time-frequency methods [5] offers some attractive alternatives due to the potential for high resolution. This must be balanced against the interference between signal components inherent in such methods. The class is described by

$$C(t, f_d) = \iint W(u, v)\Psi(u - t, v - f_d)\,\mathrm{d}u\mathrm{d}v, \tag{8}$$

with W the baseline Wigner-Ville distribution given by

$$W(t, f_d) = \int_{-\infty}^{\infty} s(t + \tau/2)s^*(t - \tau/2)\exp(-j2\pi f_d \tau)\,\mathrm{d}\tau \tag{8}$$

Various instances of Cohen's class are generated by choices of the kernel function Ψ.

We use two methods, the smoothed pseudo Wigner-Ville (SPWV) [6] and the adaptive optimal kernel (AOK) [7]. Both methods use a kernel that is essentially a low-pass filter, smoothing away high frequency interference, while retaining low frequency signal content. The SPWV is fairly simple and computationally efficient due to the simple separable kernel. The AOK method is more sophisticated as it adapts the kernel to some extent to the underlying signal.

4.0 EXPERIMENTAL RESULTS

A test was performed at Lillestrøm, Norway, 2 Jun 2003, using the German E-SAR system.

4.1 Description of Test

SAR scenes were collected over the test area at X-, L- and C-band. Several experiments were set up at the time. For the present study, a car was used as a moving target. A corner reflector was placed on the roof of the car as shown in fig. 2. The corner reflector was oriented to give maximum reflection in the general direction of the radar.

Figure 2: A standard civilian car with a corner reflector on the roof used as a moving target.

The position of the car was measured using a GPS receiver. The car path was chosen as a small road nearly in the azimuth direction. The road was in the middle of a uniform farming field to minimize clutter problems for the relevant data area. The car path was a fairly slow azimuth motion, about 5 m/s, combined with a side-to-side oscillation covering the width of the road. The aim was a linear motion in azimuth combined with a sinusoidal motion in range.

4.2 SAR Results

Fig. 3 shows a part of an X-band image collected over Lillestrøm. The image is processed by DLR e.V, Germany. Clutter is reduced using multi-look processing and the resolution is approximately 2m. Azimuth is along x-axis and range along y-axis. The bright parts in the left part of the image correspond to buildings at the site of the Norwegian Defence Establishment (NDRE) and some other institutions. The uniform part to the right corresponds to farming fields. The red rectangles show the location of the bright signature resulting from the moving target and a comparable bright signature from a building.

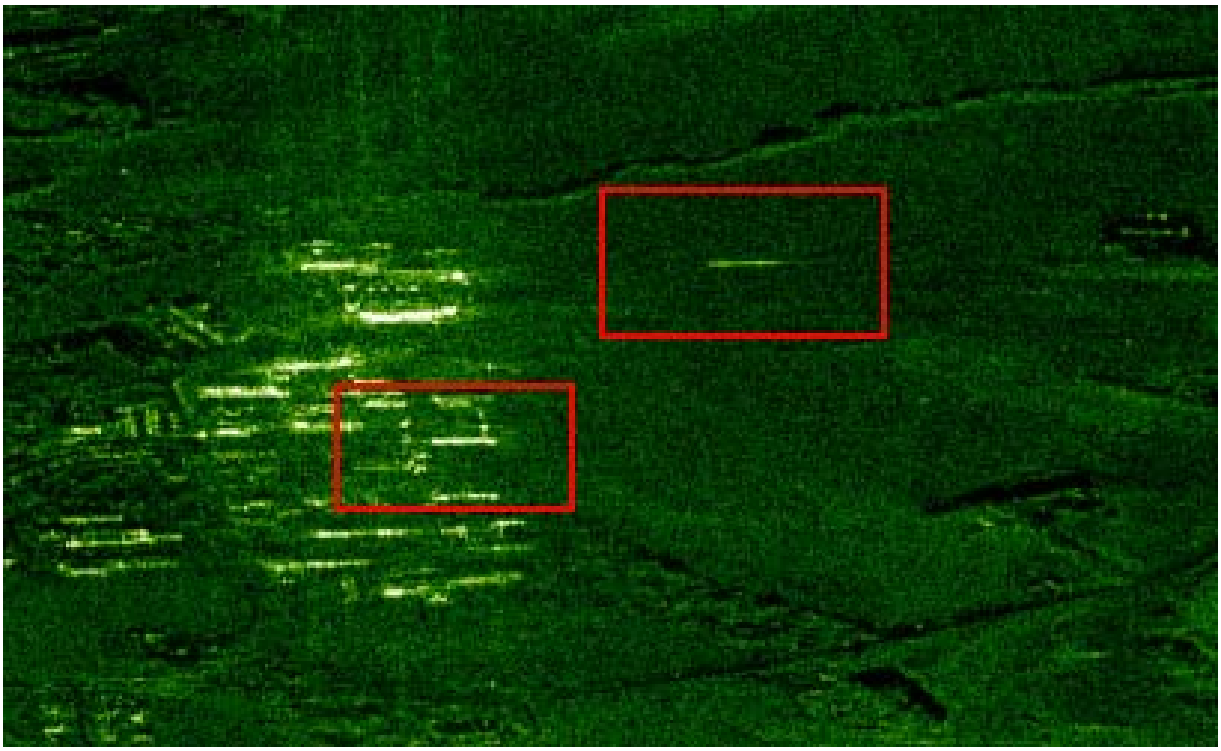

Figure 3: An X-band SAR image of an area close to Lillestrøm.
The regions within the rectangles are shown in greater detail in Fig. 4.

Fig. 4 shows close-ups of the rectangles of fig. 3.Both signatures are seen to be smears nearly in the azimuth direction as discussed in section 2.2. Taking an azimuth slice through the single-look complex representation of the signature and inverse Fourier transforming, we obtain a complex time series that may be analysed with time-frequency methods. Time-frequency signatures, calculated with the AOK method are shown in fig. 5.

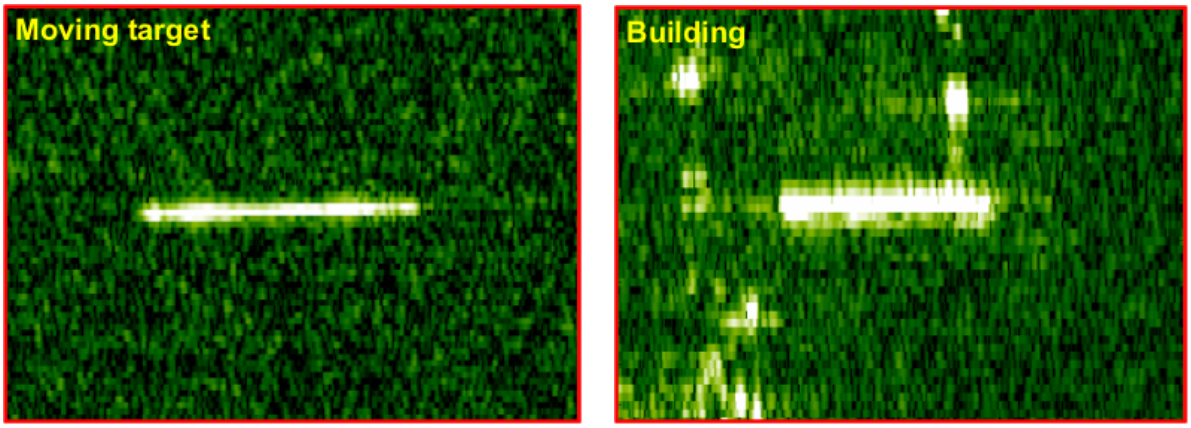

Figure 4: Close ups of the moving target and a building.

Since the ground target motion was approximately linear in azimuth, with a range oscillation superimposed, we expect the signature to be a linear chirp with sinusoidal modulations. The moving target signature in fig. 5 seems to agree well. In comparison, the building signature is different, containing

constant components, as well as wide-band time-limited components. The constant components are probably small reflectors along the edge of the building, while the time-limited wide-band components probably correspond to specular reflections. It is clear that the time-frequency signature can be used to discriminate between the staionary building and the moving target.

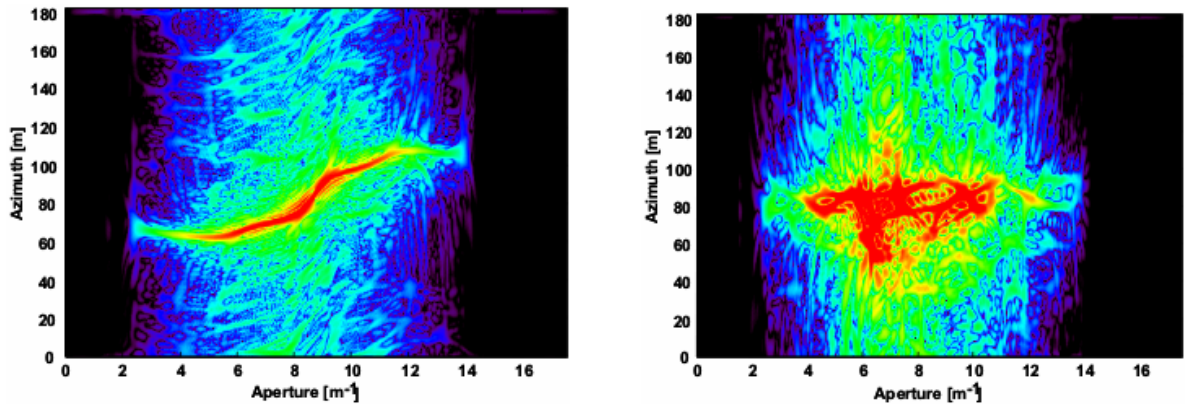

An animation of the time-frequency cube obtained by processing a number of azimuth slices shows the focused moving target moving in azimuth, in agreement with ground truth.

5.0 CONCLUSIONS

Moving targets in SAR images can be analysed and focused using time-frequency techniques. Results from a test show that the time-frequency signatures of a moving target is significantly different from the signature of a stationary building, even when the SAR image of the two are similar. Accordingly, time-frequency techniques are useful in the general problems of moving target detection, focusing and relocation.

6.0 REFERENCES

[1] Transceschetti, G.; Lanari, R.: Synthetic Aperture Radar Processing, Boca Raton, Florida: CRC Press LLC, 1999.

[2] Sullivan, R.J.: Microwave Radar: Imaging and Advanced Concepts, Norwood, Massachusetts: Artech House, Inc., 2000.

[3] Chen, V.C.; Ling, H.: Time-Frequency Transforms for Radar Imaging and Signal Analyisis, Norwood, Massachusetts: Artech House, Inc., 2002.

[4] Sparr, T.; Krane, B.: Micro-Doppler analysis of vibrating targets in SAR, IEE Proceedings on Radar, Sonar and Navigation, Vol 150, No 3, Aug. 2003, pp 277-283.

[5] Cohen, L.: Time-Frequency Analysis, Upper Saddle River, New Jersey: Prentice Hall PTR, 1995.

[6] Auger, F.; Flandrin, P.; Gonçalvès, P.; Lemoine, O.: Time-Frequency Toolbox for Use with MATLAB, 1996.

[7] Jones, D.L.; Baraniuk, R.G.: An adaptive optimal kernel time-frequency representation, IEEE Transcations on Signal Processing, Vol. 43, Oct. 1995, pp. 2361–2371.

[8] Mallat, S.: A Wavelet Tour of Signal Processing, San Diego, California: Academic Press, 1998.

[9] Sparr, T.; Krane, B.: Analysis of phase modulation caused by target motion in SAR images, Proceedings of SPIE, Vol. 5102, 2003, pp 178-188. See following page for "Header/Footer" information.